

Design and Control of Modular Compliant XY Positioning stage

Kishor K. Dhande¹, Vijayshri Mahobia², Sarika Atul Patil³, Santosh D.Sancheti⁴, Gulab Dattrao Siraskar⁵, Sandip S. Nehe⁶, Prasad Baban Dhore⁷, Rakesh Raushan⁸

¹Professor, Department of Mechanical Engineering, Dr.D.Y.Patil Institute of Technology, Pune, India.

²Assistant Professor, Department of Mechanical Engineering Wainganga College of Engineering and Management, Nagpur, India

³Associate Professor, Department of E&TC, Dr. D. Y. Patil college of Engineering, Akurdi, Pune

⁴Associate Professor, Department of Mechanical Engineering SNJB's Late Sau.K.B. Jain College of Engineering Chandwad

⁵Associate Professor, PCET's Pimpri Chinchwad College of Engineering and Research, Ravet, Pune

⁶Assistant Professor, Department of Mechanical Engineering Samarth College of Engineering, Belhe Department of Mechanical Engineering

⁷Associate Professor, Nutan Maharashtra Institute of Engineering & Technology University of Pune.

⁸Assistant Professor, Department of Mechanical Engineering, D.Y.Patil Institute of Technology, Pune, India.

Corresponding Author – rakesh.raushan@dypvp.edu.in

Article History:

Received: 11-06-2024

Revised: 23-07-2024

Accepted: 24-08-2024

Abstract:

The modular design and controller implementation of compliant XY stage having large motion range are presented. The design involves symmetric parallel kinematic configuration using compound parallelogram flexure module (CPM) with input-output decoupling properties. The architectural parameters are determined based on the performance metrics such as stiffness, resonance frequency and motion range etc. The FEA simulation predicts the range of motion of 12 mm along each working axes. A prototype is developed to assess the performances of the stage. The results exhibit the small deviation between the two working axes which reflects the better decoupled motions. The PID controller is implemented to achieve the accuracy of positioning with submicron resolution.

Keywords: Compliant, parallel kinematic, modular design, decoupling properties, motion control, translation stages.

1. Introduction

Compliant mechanisms generate precise, repeatable motions by elastic deformation of a flexible element. It offers several benefits like no friction, backlash free and lower cost. Compliant micro positioning systems gaining popularity in the domain of precision engineering and manufacturing eg. atomic force microscopy, bio cell manipulation, lithography. In precision engineering, micro positioning systems which are capable to generate large range i.e. over 10 mm, precise motion with compact size. A compact precision positioning stage allows to accommodate in limited space. Also it enables reduction in cost in terms of material and manufacturing. The kinematic scheme is determined first and architectural parameters of the stage are designed with a view to operate it in the elastic limit without fatigue failure. The material's yield strength limits the motion range which

becomes challenging to achieve large stroke. The various compliant micro positioning systems producing large range of motion are presented in. The concept of modular design of large range compliant positioning stage is proposed in . The kinematic configuration of the positioning stages is classified in two categories i.e. serial and parallel configuration. Some research efforts are devoted to the serial configuration. In serial kinematic scheme, micro positioning have been mounted vertically on the other stage, serial mechanism has drawbacks of natural frequencies, parasitic motions, increased inertia due to moving mass, bulkiness etc. . As compared to serial configuration, parallel configuration is widely used in most of two degree of freedom micro motion stages because it offers advantages such as high payload capacity, symmetrical structure, lower moving mass and higher stiffness . Nano positioning stage can provide a motion resolution at nanometre scale. Such high resolution depends upon the type of actuators and sensors. Most of micro/nano precision stages uses piezoelectric stack actuators (PSA). The drawback of PSA is limited motion range in microns. Various lever amplifying mechanisms are used to amplify the desired motion . To achieve large range of motion, ball screw drives are commonly used . It generates large motion range but possess nonlinearity due to friction which affect the positioning accuracy adversely So drives such as electromagnetic actuators , magnetic levitation actuators and voice coil motors have been employed . Various types of flexure hinges are utilized to construct the stage . To obtain large range, beam flexure is most commonly used. The large stroke needs long and thin flexure. The length of flexure is limited by the compact size and manufacturing constraints. So the challenging task is to design the stage with the objective of large motion range and compactness. Several design configurations have been developed to resolve the issues. Hence the compliant XY stage is designed using compound parallelogram module as basic building block . The large range translational motion is achieved by multistage compound parallelogram flexure (MCPF) . After fabrication of prototype, precise positioning depends upon the control methods. The number of vibration modes is observed due to low value of damping of the stage. Hence the system is identified using high order controller model. The linear second order is preferred for effective implementation of the control algorithm. Different control methods have been used to achieve robust performances in the presence of disturbances and dynamic model uncertainties. The proportional-integral-derivative (PID) is most commonly used control in various industrial domains . PID control possesses weak robustness against system nonlinearities and uncertainties. Various controller approaches have been adopted to achieve better performance of micro-positioning system . In the current research work, modular design of compliant XY stage with voice coil actuator is presented. The paper is organized as follows. concept of modular design and kinematic configuration is explained in section 2. The Finite element analyses (FEA) is carried out to evaluate the static and dynamic performances in section 3. The prototype development and experimental tests are demonstrated in section 4. The open loop static and dynamic performances are demonstrated in section 5. The system identification is implemented in section 6. The PID control scheme implementation and the closed loop set point positioning, sinusoidal positioning performances provided in section 7. In section 8, the results are discussed and in the last, concluding remarks are provided.

2. Design of Modular XY stage with compound parallelogram module (CPM)

To design translational XY stage with decoupled motions, 2-PP parallel symmetric kinematic configuration is employed. The architecture utilizes the 2 prismatic joints (i.e.2PP) as active joints in the outer parallelogram and 4-PP joint as passive joint in the inner parallelogram. Single layer leaf flexure is adopted as the flexure unit. The modular design divides the micro-positioning system into four distinct components such as first stage, intermediate, flexure and the motion stage. These components can be independently fabricated and assembled to obtain the modular compliant XY micro motion stage. Fig.1.shows translational motions along X and Y directions along with limited kinematic coupling.

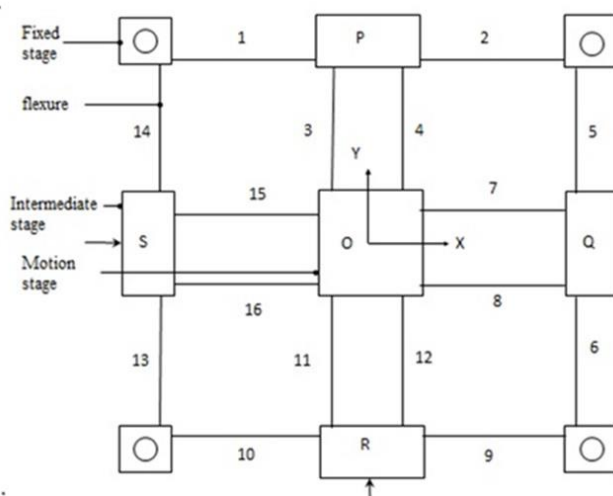


Fig.1 Schematic diagram

2.1 Parametric Design

The key architectural parameters such as length, height and thickness (l, w, t) of flexure are carefully designed in order to achieve the desired performances i.e. Range of motion, equivalent stiffness and resonant frequency. The four mounting holes are designed to form square symmetric parallel configuration of the stage. The stage exhibits limited kinematic coupling between the two axes resulting in well decoupled motions. The parametric design is carried out by considering the stress and buckling load constraints. In parametric design only bending deformations are considered by neglecting the axial deformation of the leaf flexures. Table 1 and Table 2 provides the architectural and material parameters of the stage.

Table 1: The Architectural parameters of the stage

Parameter	Symbol	Value (mm)
Length of the flexure	l	75
Width of the flexure	w	15
Thickness of the flexure	t	0.8
Distance between mounting holes	c	250

Table 2: The Material parameters of the stage

Material	Density (ρ) Kg/m ³	Poisson's ratio (μ)	Yield stress (σ_y) Mpa	Young's modulus (E) Gpa
Al alloy T6-6061	2700	0.3	276	2700

2.2 Motion Range consideration

The maximum range for single axis translation motion of the XY stage is determined using the equation 1.

$$R_{max} = \frac{2\sigma_y l^2}{3Et} \text{----- (1)}$$

Where R_{max} = motion range in each working axes which results in workspace of $2 R_{max} \times 2 R_{max}$, σ_y = permissible yield stress of material, l , t = length, thickness of the beam flexure, E = Young's modulus of the material. The main architectural parameters are as shown in table 1. The actual workspace should lie within the workspace calculated above for safety of material. The parameters are designed to fulfil the following condition given by the equation 2.

$$D_{max} \leq \frac{2\sigma_y l^2}{3Et} \text{----- (2)}$$

In which D_{max} = Maximum reachable workspace of the stage.

2.3 Stiffness and actuation force consideration

Due to functional requirement of large range of motion, Voice coil actuators (VCA) with maximum actuation force, $F_{VCA}=194.6$ N is used for actuation. The equivalent stiffness of the mechanism is obtained by considering symmetry of the configuration given by the equation 3.

$$K_{stage} = \frac{2Ewt^3}{l^3} \text{----- (3)}$$

The stiffness determines the force -displacement relation given by the equation 4.

$$F_{in} = K_{stage} X_{out} \text{----- (4)}$$

Where F_{in} = input or actuation force applied at the intermediate stage, X_{out} = displacement at the motion stage. The force of voice coil actuator should be greater than the required input force.

$$F_{in} \leq F_{VCA} \text{----- (5)}$$

$$\frac{2Ebt^3}{l^3} X_{out} \leq F_{VCA} \text{ ----- (6)}$$

2.4 Buckling effect consideration

Leaf spring flexures with relative higher length to thickness ratio are used for architecture of stage. These flexure is subjected to elastic buckling or bending under the axial compressive loads which results into reduction in the motion transmitted to moving platform. So the buckling effect can be eliminated by the architecture design. Theoretically buckling load is given by the equation 7 .

$$P = \frac{\pi^2 EI}{l_e^2} \text{ ----- (7)}$$

Where $I = \frac{wt^3}{12}$ is the moment of inertia of the cross section of beam flexure, l_e is the equivalent flexure length which varies from $0.5x l$ to $2x l$ depends upon boundary conditions. The flexure beam is considered with fixed-fixed boundary conditions hence $l_e = 0.5 \times l$. The crippling load is as follows

$$P_{cr} = 2P = \frac{8\pi^2 EI}{l^2} \text{ ----- (8)}$$

To avoid buckling failure of flexure beam, following condition needs to satisfied

$$F_{VCA} \leq P_{cr}$$

$$F_{VCA} \leq \frac{2\pi^2 Ewt^3}{3l^2} \text{ ----- (9)}$$

$F_{VCA} \leq 646.31N$ To avoid buckling failure, buckling force must be greater than the maximum actuation force i.e. 194.6 N.

3. FEA Analyses

The FEA through ANSYS software is used to validate the analytical models for assessment of static and dynamic performances. The FEA results validate the motion range of 12 mm along the working direction and the maximum stress developed in the flexure is less than permissible stress of the material. The prestressed modal analysis results predict the natural frequencies of the vibration and the corresponding shapes as shown in fig. 2. Table 3 shows first three resonance frequencies of the stage.

Table 3: The first three resonant frequencies

Method	X/Y axes (Hz)	Z axes (Hz)
Analytical	16	130
FEA	20	135
Experiment	15	128

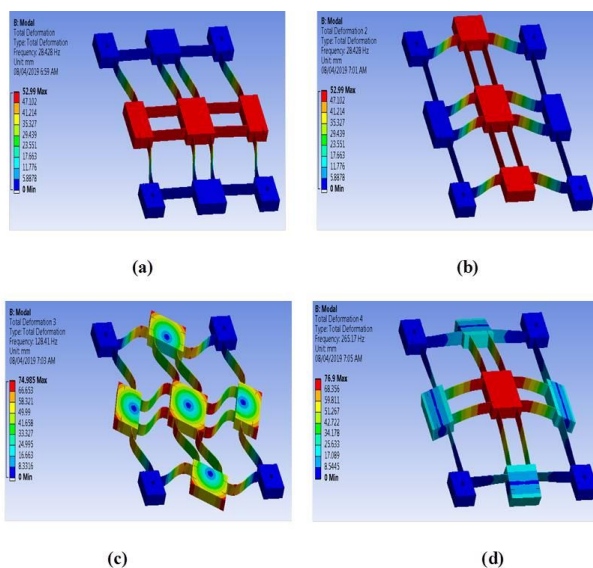
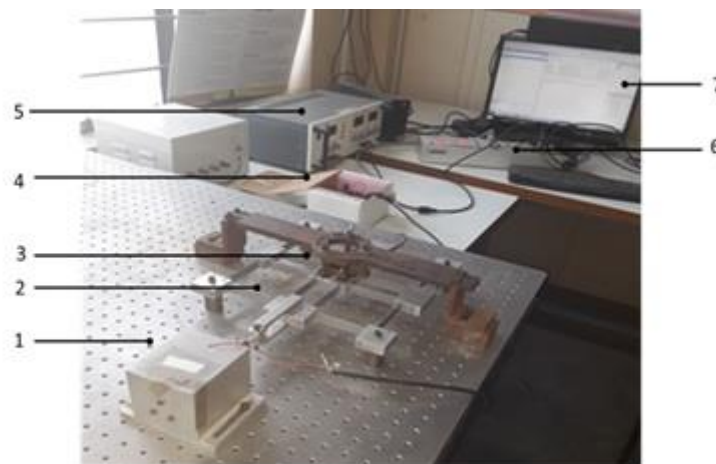


Fig. 2 The modes of vibration (a) First (b) Second (c) Third (d) Fourth

4. Prototype development and test setup:

The experiment test up shown in fig.3 consists of a Dspace device DS1104 controller board with A/D and D/A converter board interface with computer is used as real time control unit. The four channel linear current amplifier from Quanser systems is used to drive the voice coil actuator (VCA 32-30, rated force is 60 N) and the position output of the stage is measured by linear optical encoder RELM scale, 50 nm resolution from RENISHAW Inc. The micro motion stage and optical encoder are mounted on isolation table from Newport Inc. to avoid the effect of external vibration.



1- Voice coil actuator, 2- Compliant stage, 3- Linear optical encoder, 4- Linear current amplifier, 5- DC power supply, 6- Dspace DS 1104 , 7- Desktop

Fig. 3 Experimental test rig

5. Open loop performance tests

5.1 Voltage-displacement test

A sinusoidal voltage signals at low frequency 0.5 Hz are applied to each VCA and the output displacements along two directions are measured using linear optical encoder. CA 1 is driven with $\pm 1.4V$ voltage amplitude, stage displacement of 12 mm is observed in X axes as shown in fig. 4. The parasitic motion of $10 \mu m$ is depicted in Y direction. So the design objective with large range of motion with decoupled motion is achieved. In open loop test, voltage –displacement curve is nonlinear due to hysteresis effect. So it needs to apply control methods to achieve the precise positioning.

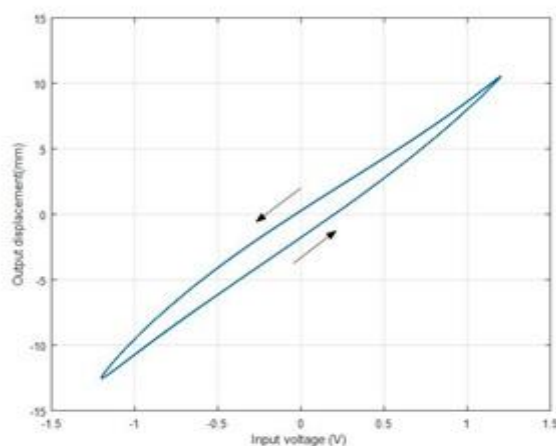


Fig.4 Hysteresis in voltage –displacement curve.

5.2 Open loop step response test

Step response of stage is evaluated without feedback control as shown in fig. 5. The stage produces settling time of 1.8 sec with 4.6 % overshoot. It shows that the stage has slow response with maximum steady state error of 97%.

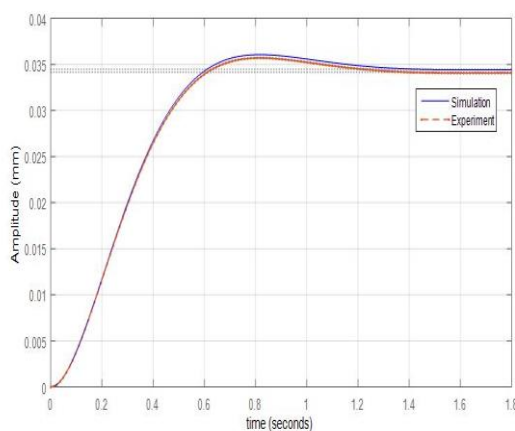


Fig.5 Open loop step response

5.3 Frequency response test

The open loop dynamics performance is obtained by frequency response test. In this test, sinusoidal signal of 1.4 V amplitude and frequency upto 50 Hz is implemented by the digital to analog (DAC) channel of the Dspace DS 1104 unit and supplied to linear current amplifier which drives the VCA. The frequency response is obtained by performing spectral analysis. The frequency response in terms of magnitude and phase plots are demonstrated in fig. 6. In open loop test, each VCA is driven independently without feedback control applied to it.

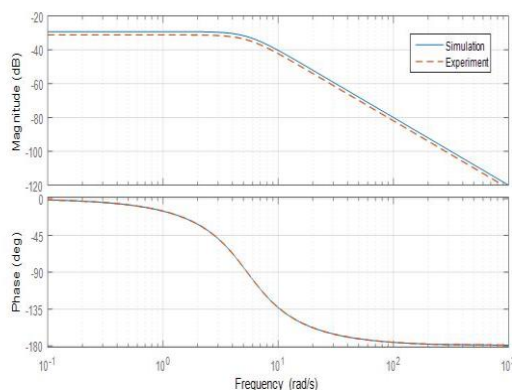


Fig.6 Open loop frequency response

5.4 Open loop sinusoidal positioning test

In open loop test, each VCA is driven independently without feedback control applied to it. A sinusoidal signal of amplitude 1.4V at frequency 5Hz is applied to the VCA. Fig.7 shows open loop sinusoidal response having actual amplitude of 0.03 mm showing large positioning error.

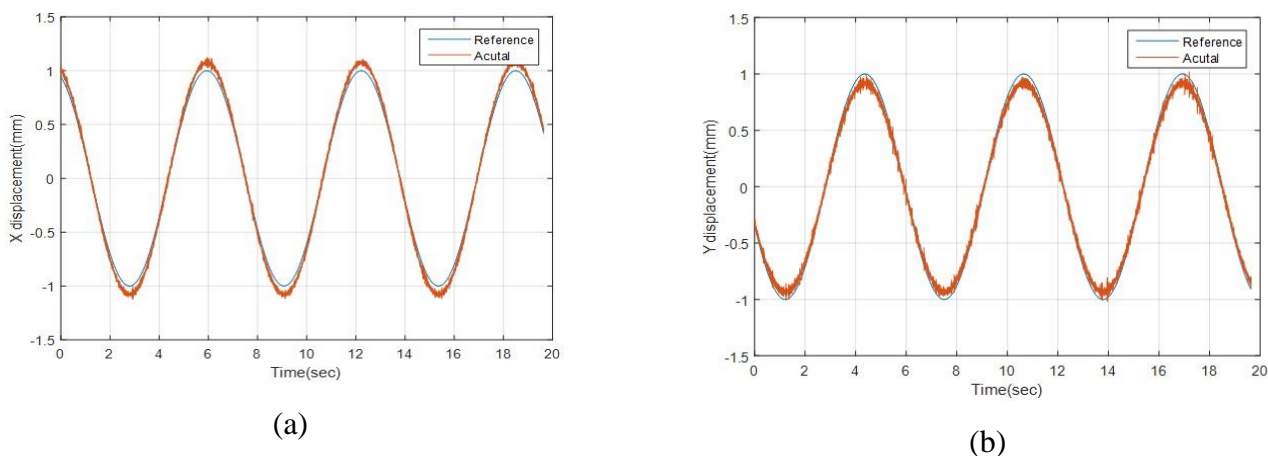


Fig.7 Open loop sinusoidal response along a) X axis b) Y axis.

5.5 Open loop trajectory tracking Test

To evaluate the planar motion capabilities of the stage, elliptical trajectory tracking test is carried out. The actual and reference input trajectories are plotted as shown in fig.8. The results depicts the better tracking performance with error of 6µm in both X/Y axes.

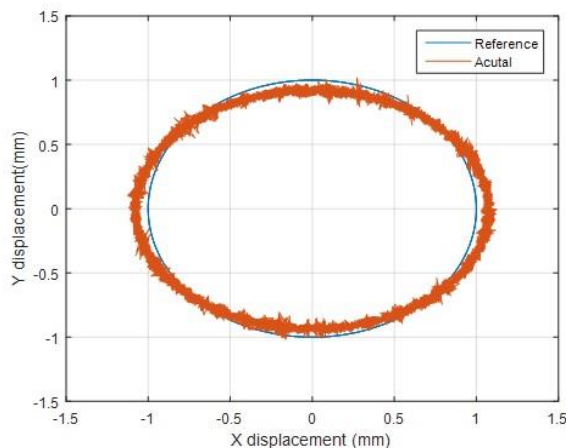


Fig.8 Open loop elliptical trajectory tracking performance of the stage

6. System Identification

Transfer function is identified from the experimental frequency response of the system as follows

$$G(s) = \frac{1}{0.35s^2 + 2.64s + 10.15}$$

The transfer function model approximates the dynamic behavior upto 50 Hz. The model captures the system dynamics at high frequencies. The dynamics model parameters are obtained as M=0.35 Kg, C=2.64 N-S/mm, K=10.15 N/mm respectively.

7. Implementation of the Proportional –Integral-derivative (PID) control

The PID control is applied for minimizing the error in open loop performances to obtain the precise motion and the closed loop performances are evaluated. Fig.9 shows the schematic diagram of control scheme.

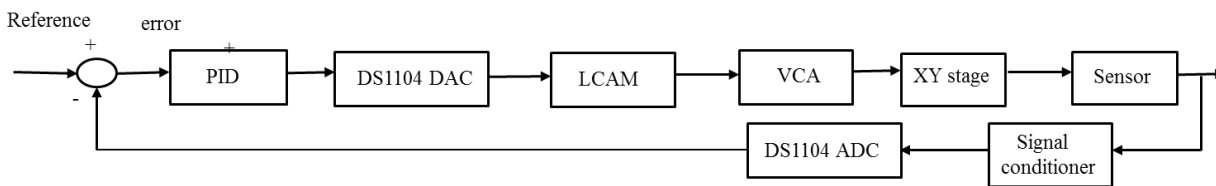


Fig.9 Schematic diagram of control scheme

7.1 Closed loop positioning performance tests

7.1.1 Closed loop step response test

Step response of micro-positioning system is evaluated using PID controller as shown in fig.10. The PID controller produces settling time of 0.03 sec with no overshoot. It shows that the stage has fast response as well as minimal steady state error. The average value of steady state error of 2 μm is produced by the stage. The PID gains by trial and error are K_p = 600, K_i= 350 and K_d=340 respectively.

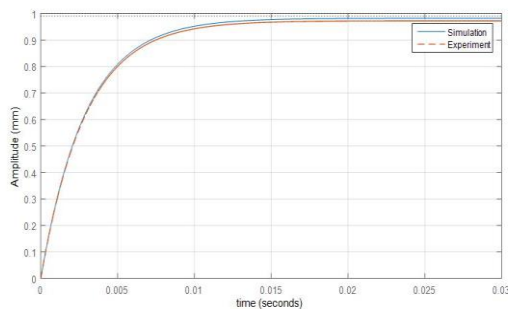
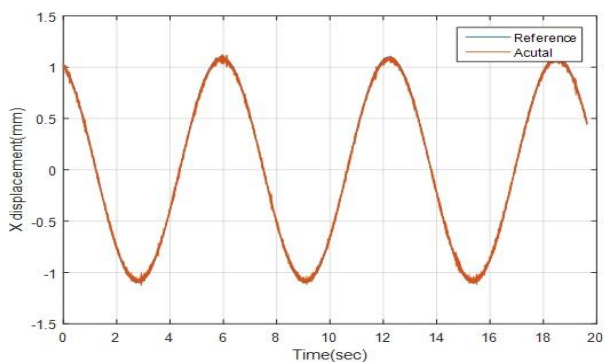


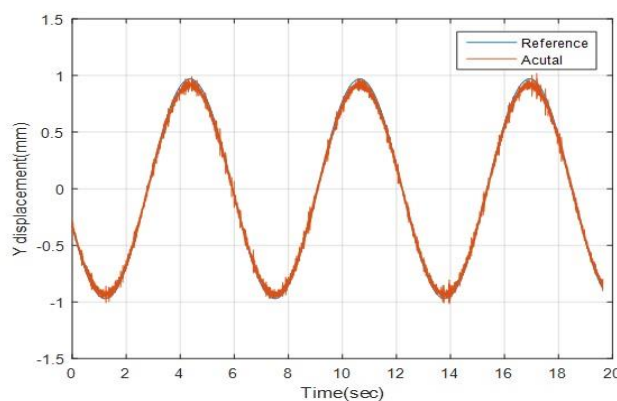
Fig.10 Closed loop step response

7.1.2 Closed loop sinusoidal response test

The sinusoidal motion tracking with voltage amplitude 1.4 V is carried out. Fig.11 (a) and (b) Shows the tracking results along X and Y axes in which entire motion range is covered by the micro positioning stage. The accurate positioning is observed. The PID gains by trial and error are $K_p = 600, K_i = 350$ and $K_d = 340$ respectively.



(a)



(b)

Fig.11 Closed loop sinusoidal response along a) X axis b) Y axis

7.1.3 Closed loop Frequency response test

The closed loop frequency response is obtained by implementing the PID controller. The sinusoidal signals of the amplitude 1.4 V and range of frequency from upto 50 Hz. The Bode plots of PID control system is shown in fig.12. The phase difference of 90° occurs within -3 dB bandwidth which results in tracking error. The resonant frequencies along each axes to be 15 Hz is obtained. It is observed that experimental frequencies are slightly lower than frequencies obtained by simulation. The deviation is due to moving mass of the coils of the VCAs which is not included in FEA simulations. The stage shows identical dynamic properties as the same resonant frequencies are observed along the working axes.

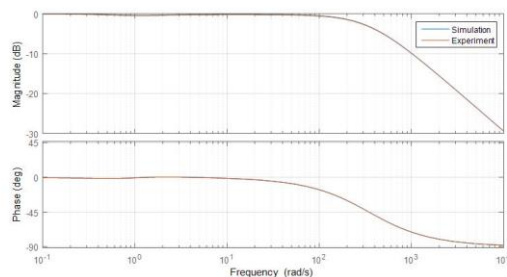


Fig.12 Closed loop bode diagram

7.1.4 Closed loop elliptical trajectory tracking Test

The PID control is implemented to demonstrate the planar motion capabilities of the stage in the closed loop elliptical trajectory tracking test. The actual and reference input trajectories are plotted as shown in fig.13. The results depicts the better tracking performance. The PID gains by trial and error are $K_p = 600$, $K_i = 350$ and $K_d = 340$ respectively.

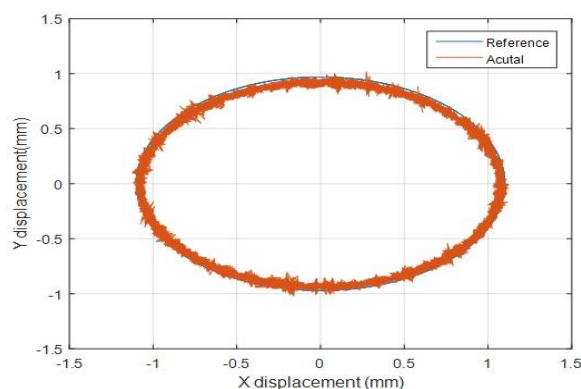


Fig.13 Closed loop elliptical trajectory tracking performance of the stage

8.Result Discussions

The comparison between the step performance of the XY stage without and with feedback control is shown in table 4. The open loop step responses shown in figure 5 has steady state error of 6 microns and overshoots of 4.6% whereas the closed loop response shown in fig. 10 is very fast with minimal steady state error less than 2 microns and without overshoot. In case of open loop sinusoidal response shown in fig. 7 (a) and (b), point to point positioning error of 6 microns is observed whereas closed loop sinusoidal response shown fig.11 (a) and (b) shows better point to point positioning. The open loop frequency response i.e. Bode plot shown in fig.6 shows negative dc gain with very low resonant frequency whereas closed loop bode plot shown in fig.12 has the resonant frequency of 15 Hz at -3 dB magnitude and at the phase lag of 30° is observed. There are 5% deviations between the simulation and test results. The deviations are due to inaccuracy of the simulation model or due to hardware constraints in the test results. The simulation results are 5% larger than test results.

Table 4 Openloop and closed loop step response parameters

Parameter	Peak amplitude	Rise time (sec)	Settling time(sec)	% overshoot
Open loop	0.035	0.39	1.8	4.6
Closed loop	0.99	0.0068	0.03	-

9. Conclusion

The design and PID control implementation of modular compliant XY micro-positioning stage have been presented. The numerical result depicts workspace of 12 mm X 12 mm which then validated by the experiment. The architectural parameters are obtained with the main objective of large range of motion while compromise in the resonance frequency under the constraints of stress and buckling effect. The test results reveal that the stage has the decoupled motions along the working axes. The results depicts similar dynamics characteristics in two axes with same resonance frequency of 15 Hz. With implementation of PID control in two axes, better positioning accuracy is obtained. The tracking error less than $2 \mu\text{m}$ is accomplished. The experiment results validate the better positioning capabilities of the developed stage with submicron accuracy.

Data availability statement: All the data related to the research article is available

References

- [1] L.L Howell, Compliant mechanisms, Wiley, New York, 2001.
- [2] A Sinno, Ruauax, Enlarged atomic force microscopy scanning scope: Novel sample holder device with millimetre range. Rev. sci. Instru. 78 (9), 095107, 2007.
- [3] N. I Jamadar, S. B. Kivade, & Rakesh Raushan (2018). Failure Analysis of Composite Mono Leaf Spring Using Modal Flexibility and Curvature Method. Journal of Failure Analysis and Prevention, 18, 782–790. <https://doi.org/10.1007/s11668-018-0418-4>
- [4] Rakesh Raushan, K.K. Dhande, N.I. Jamadar (2024). Mathematical modelling for failure analysis of composite drive shaft using modal flexibility and curvature method. Communications on applied nonlinear analysis, 31(1s), 42–55. <https://doi.org/10.52783/cana.v31.555>
- [5] 5.M.Gauthier, Piat, Control of a particular micro position system applied to cell micro-manipulation, IEEE Trans. Automation Science and Engg, 3(3), pp-264-271, 2006.
- [6] D.J Lee, K.Kim, H.G Choi, Robust design of novel three axis fine stage for precision positioning in lithography, Proc. Inst. Mech. Eng, Part C-I, Mech. Engg. Sci: 224(4), pp-877-888, 2010.
- [7] Rakesh Raushan, K.K. Dhande, N.I. Jamadar & Prateek D. Malwe (2022), Material characterization, design and analysis of CF/PA66 drive shaft with high strength carbon steel, 51-58 <https://doi.org/10.1016/j.matpr.2022.03.512>
- [8] Rakesh Raushan, K.K. Dhande, N.I. Jamadar (2024) Modal analysis of carbon fibre reinforced polyamide66 drive shaft using analytical and finite element approach International Journal on Interactive Design and Manufacturing (IJIDeM), 1-16. doi.org/10.1007/s12008-024-01854-7
- [9] Qingsong Xu, Design and implementation of large range compliant micro-positioning system, John Wiley and sons Inc. Singapore, 2016.
- [10] 10.S.Jadhav, K.Dhande, S.Deshmukh, Design and evaluation of compliant modular XY positioning stage, Australian journal of Mech. Engg. 2020, DOI: 10.1080/14484846.2020.1816709.
- [11] D.M.Kim, D.W.Kong et.al, Rev.Sci.Instru. 76, 073706, 2005.
- [12] Y.M.Li, Q.Xu, IEEE Trans. Robotics and automation 25, 645, 2009.
- [13] Q.Yao, Dong, P.M.Ferreira, Design ,analysis, fabrication and testing of a parallel kinematic micro-positioning stage, Int.J.Mach.Tools.Manuf., 47(6), pp-946-961, 2007.

- [14] 14.Rakesh Raushan, K.K. Dhande, N.I. Jamadar(2024) Design, Development and Manufacturing of Carbon fibre Nylon 66 Drive shaft of Passenger Vehicle Journal of Physics: Conference Series 2763 (2024) 012007,1-9 doi:10.1088/1742-6596/2763/1/012007
- [15] 15.Amit Chaudhary, Ashish Ekatpure, Dinesh Burande(2023)Exploring Beishan Granite Damage Patterns: Statistical Analysis of Single and Multiple Loading via Acoustic Emission Techniques Panamerican Mathematical Journal ISSN: 1064-9735 Vol 33
- [16] 16.Xu Q, Li Y., Analytical modeling, optimization and testing of compound bridge type compliant displacement amplifier, Mech.Mach.theory, 46(2), pp-183-200, 2011.
- [17] 17.J.J Kim, Y.M. Choi, A millimeter range flexure based nan positioning stage using self-guided displacement amplification mechanism, Mech.Mach.theory, 50, pp-109-120, 2012.
- [18] J.Otsuka, S.Ichikawa, Development of a small ultra-precision positioning device with 5 nm resolution, Measurement of science and technology, 16(11), 2186, 2005.
- [19] D.H.Kim, M.G.Lee, A super elastic alloy micro gripper with embedded electromagnetic actuators and piezoelectric force sensors: A numerical and experimental study, smart materials and structure, 14(6), pp-1265-1272, 2005.
- [20] 20.S.erna, W.J.Kim, Six axis nan positioning device with precision magnetic levitation technology, IEEE/ASME Trans.on mechatronics, 9(2), pp-384-391, 2004.
- [21] 21.Q.Xu, Design and implementation of a novel rotary micro-positioning system driven by linear voice coil motor, The review of scientific instruments, 84(5), 055001, 2013.
- [22] Y.K.Yong, T.F.Lu, Review of circular flexure hinge design equations and derivation of empirical formulations, precision engineering, 32(2), pp-63-70, 2008.
- [23] S.Awtar, G.Parmar, Design of a large range XY nan positioning system, Proc.of ASME, 2010 Int.Design Engineering Tech.conf., Montral, Canada, 2010.
- [24] Q.Xu, New flexure parallel kinematic micro positioning system with large workspace, IEEE transactions on Robotics, 28(2), pp-478-491, 2012.
- [25] Jaju, S.B., Charkha, P.G., Kale, M., Gas metal arc welding process parameter optimization for AA7075 T6, Journal of Physics: Conference Series 1913 (1), 2021.
- [26] M.Jasench, M.U.Lamperth, Investigations into the stability of a PID controlled micro positioning and vibration attenuation system, smart mat.structure, 16(4), pp-1066-1075, 2007.
- [27] S.Q.Lee, Y.Kim, Continuous gain scheduling control for micro-positioning system: Simple, robust and no overshoot response, control Eng.pract, 8(2), pp-133-138, 2000.
- [28] 28.J.Dong, S.M.Salapaka, Robust control of a parallel kinematic nano positioner, Journal of Dynamic system, Meas.control, 130(4), 041007-1-041007-15, 2008.
- [29] 29.X.Tan, J.S.Baras, Adaptive identification and control of hysteresis in smart materials, IEEE Trans.Automatic control, 50(6), pp-827-839, 2005.
- [30] 30 .Rohit Jadhao, Vijayshri Mahobiya, Prasad Baban Dhore, Roundal Vijay Baburao, Gorane Prathamesh Sudhakar, Vijaykumar Javanjal, Mangesh Kale, Pranav Charkha, Experimental Analysis of Mechanical Tests on a Plate Composed of Banana Fibre, Communications on Applied Nonlinear Analysis, Vol. 31 No. 1s (2024), Page No.141 –150. <https://doi.org/10.52783/cana.v31.562>.
- [31] Ashwin Raj Suresh, R Venkatasubramanian, L Hussien Jasim, MP Santhoshkumar, Saurabh Aggarwal, Mangesh Kale, Integrating Hydrogen Energy Storage into Urban Mobility Solutions, 2024, E3S Web of Conferences, Volume - 540, Pages 11009